Dynamics of Tropical Cyclone Intensification: Deep Convective Cyclonic "Left Movers"

WALLACE A. HOGSETT* AND STACY R. STEWART

NOAA/NWS/National Hurricane Center, Miami, Florida

(Manuscript received 10 October 2012, in final form 26 July 2013)

ABSTRACT

Deep convective processes play an important role in tropical cyclone (TC) formation and intensification. In this study, the authors investigate the interaction between discrete buoyant updrafts and the vertically sheared azimuthal flow of an idealized TC vortex by adapting the updraft–shear dynamical framework to the TC. The authors argue theoretically that deep updrafts initiating near the TC radius of maximum wind (RMW) may propagate with a component left of the mean tangential flow, or radially inward toward the TC center. Results suggest that these unique TC updrafts, or ''left movers'' with respect to the mean azimuthal flow, may play an active role in TC intensification.

The notion that updraft-scale convection may propagate with a component transverse to the mean flow is not at all new. Cyclonic midlatitude supercell thunderstorms often deviate from their mean environmental flow, always to the right of the environmental vertical shear vector. The deviant motion arises owing to nonlinear interactions between the incipient updraft and the environmental vertical shear. Although significant differences exist between the idealized TC considered here and real TCs, observational and high-resolution operational modeling evidence suggests that some intense TC updrafts may propagate with a radially inward and right-of-shear component and exhibit structural characteristics consistent with theory.

The authors propose that left movers constitute a unique class of intense TC updrafts that may be favored near the TC RMW where local vertical shear of the TC azimuthal winds may be maximized. To simulate these left movers in a realistic way, mesoscale TC forecasting models must resolve nonlinear interactions between updrafts and vertical shear.

1. Introduction

Tropical cyclone (TC) intensity change often results in large forecast errors when it occurs rapidly (Rappaport et al. 2009). Rapid intensification (RI) presents a tremendous hazard if coastal populations are underprepared, and it is among the most significant challenges facing operational TC forecasting centers. Increasing RI forecast skill is one of the primary goals of the ongoing Hurricane Forecast Improvement Program (HFIP).

Despite an ongoing technological revolution that has ushered in higher-resolution TC-specific dynamical models as routine forecast aids, intensity forecast skill has improved little contemporaneously (Cangialosi and Franklin 2011). Factors that limit the intensity skill of the dynamical models include inadequate physical parameterizations of small-scale physical processes (Sampson et al. 2011), limited observational data, and grid spacing that remain too coarse to fully resolve convective processes. A more complete physical understanding of the small-scale processes ongoing within the TC inner core is a prerequisite to both model and operational intensity forecast improvements.

Typically, the strongest winds associated with mature TCs occur in the lower troposphere near the eyewall, and the magnitude of the winds generally decreases with height and radius. It is well known that as the TC intensifies, the radius of maximum winds (RMW), which is closely associated with the eyewall, tends to contract (Shapiro and Willoughby 1982; Willoughby 1990). The eyewall contraction process is observed frequently (Black and Willoughby 1992; Corbosiero et al. 2005) and more

* Current affiliation: NOAA/NWS/Weather Prediction Center, College Park, Maryland.

Corresponding author address: Wallace A. Hogsett, NOAA/NWS/National Hurricane Center, 11691 SW 17th St., Miami, FL 33165-2149.
E-mail: wallace.a.hogsett@noaa.gov

DOI: 10.1175/JAS-D-12-0284.1

recently has been modeled successfully at cloud-permitting resolution (Liu et al. 1999; Chen et al. 2011). However, while it is established that eyewalls do contract, the dynamics of the contraction has yet to be explored fully.

Many TC evolutionary features, including eyewall contraction, can be investigated in an axisymmetric framework (Willoughby et al. 1984), but it has long been known that asymmetric deep convective elements often occur during and may play a role in TC intensification (e.g., Riehl and Malkus 1961). Hendricks et al. (2004) coined the term ''vortical hot tower'' (VHT) to describe particularly vigorous, deep, helical, and buoyant updrafts that are the preferred mode of convection near developing TCs. VHTs are ubiquitous features of TCs and are generally considered to play some role in the genesis and intensification of TCs owing to the enormous amount of vertical vorticity generated by stretching in their updrafts. Such intense, updraft-scale convective bursts occur not only in the formative stages of the TC but also have been implicated in the RI of existing TCs (Black et al. 1996; Guimond et al. 2010).

Although many studies, both modeling and observational, depict VHT-like convective bursts in the inner core of TCs, relatively little is certain about the interconnections between updraft-scale dynamics and TC evolution (i.e., the complex multiscale problem that is TC intensification). The inner core of the TC remains an extremely difficult location to acquire observations, so although these deep and sometimes long-lived convective bursts may be partially observed by aircraft and satellite, the available observational data have not yet yielded a complete understanding of their behavior.

Of particular importance to this study is that when intense updrafts develop and evolve near the eyewall of an intensifying TC, they always do so in a vertically sheared vortex-scale environment. That is, in a warm-core vortex the tangential winds are greater in the lower troposphere than in the mid- and upper troposphere. It is well known that sufficient vertical shear can dramatically impact the evolution of updraft-scale moist convection (e.g., Klemp 1987) by causing updrafts to deviate from their mean environmental flow, to split, and to acquire intense rotation through nonlinear interactions with their sheared local environment. Much research has been conducted to understand these midlatitude supercell thunderstorms.

In fact, quite a lot of research has been conducted to understand supercell thunderstorms in the TC periphery, both offshore (e.g., Eastin and Link 2009) and after landfall (e.g., McCaul 1991). These studies have found similarities between TC rainband supercells and midlatitude supercells, but the supercells occurring in the TC periphery are generally shallower (McCaul 1991). Numerical simulations confirm that the dynamics of these miniature supercells (Eastin and Link 2009) is similar to midlatitude supercells (McCaul and Weisman 1996).

However, likely because of limited observational tools to investigate the TC inner core over the ocean during intensification, less is known about the deeper inner-core updrafts (Houze 2010) that more likely contribute to TC intensity changes (Vigh and Schubert 2009). Convection in the TC inner core often occurs in deep convective bursts that comprise only a small percentage of eyewall area (Riehl and Malkus 1961; Braun 2002) but extend to (Riehl and Malkus 1958), and often overshoot (Monette et al. 2012), the tropopause.

In this study we aim to provide new insight into the physical processes ongoing within deep updrafts of the TC inner core. To this end, we extend the updraft–shear interaction theory, summarized by Klemp (1987), to the TC inner core and propose a possible role for a certain class of intense TC updrafts in TC intensification. We focus specifically on intense updrafts that occur near the eyewall and RMW and have been implicated in efficient vortex spinup (Hack and Schubert 1986; Vigh and Schubert 2009). By focusing on the updraft and its local environment, we seek to shed light on the evolution of these mysterious features of the TC inner core.

The study is organized as follows. The subsequent section reviews previous research on updraft–shear interactions for midlatitude updrafts. Section 3 extends the midlatitude dynamic framework for TC updraft–shear interactions and presents hypotheses on the role of certain VHTs in TC intensification. Section 4 presents some observational and numerical simulation results to support the hypotheses. A discussion and forecasting implications are provided in the final section.

2. Updrafts in vertical shear

In this section we review idealized updraft dynamics, as it is understood for midlatitude updrafts that develop in unidirectional shear (Rotunno and Klemp 1982; Weisman and Rotunno 2000). We constrain the discussion to unidirectional vertical shear because the relevant dynamics can be derived from this simple state. Klemp (1987) provides an overview of the physical processes associated with the formation and evolution of rotating updraft-scale thunderstorms.

Though much of the existing literature uses Cartesian coordinates, here we present the updraft-scale dynamics in cylindrical coordinates to ease the forthcoming comparison to the TC. In this framework, one may view the North Pole as the origin (Fig. 1a) and envision an eastward-moving updraft that propagates down azimuth at a constant radius. Any northward (southward) deviation

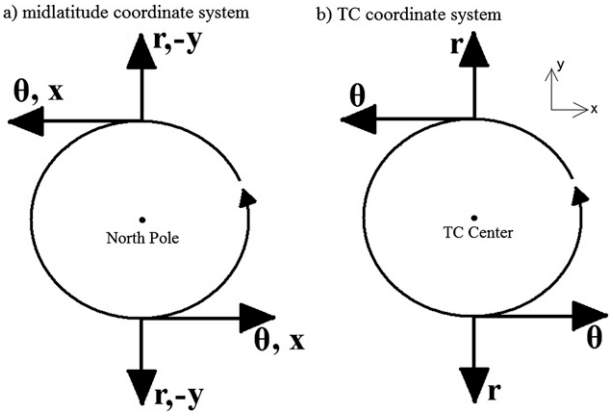

FIG. 1. Cylindrical coordinate system used for horizontal flow in the (a) midlatitudes and (b) TC. In (a), the origin is the North Pole, and in (b) the origin is the TC center. Cartesian coordinates are included for reference, and the orientation of the Cartesian and cylindrical coordinate systems is invariant only in (a).

can be viewed as radially inward (outward). The orientation of the cylindrical coordinate system with respect to the Cartesian system is invariant for the midlatitude case. Certainly this coordinate framework is for demonstration purposes only, since we disregard Earth's curvature. Following Rotunno and Klemp (1985), ignoring friction, Earth's rotation, and density gradients, the vertical vorticity (ζ) equation in cylindrical coordinates is

$$\frac{d\zeta}{dt} = \boldsymbol{\omega}_H \cdot \nabla_H w + \zeta \frac{\partial w}{\partial z}, \tag{1}$$

where

$$\boldsymbol{\omega} = (\xi, \eta, \zeta) = \left(\frac{\partial w}{r\partial\theta} - \frac{\partial v_\theta}{\partial z}\right)\hat{r} + \left(\frac{\partial v_r}{\partial z} - \frac{\partial w}{\partial r}\right)\hat{\theta} + \left(\frac{\partial r v_\theta}{r\partial r} - \frac{\partial v_r}{r\partial\theta}\right)\hat{k}$$

and

$$\mathbf{V} = (v_r, v_\theta, w) = v_r\hat{r} + v_\theta\hat{\theta} + w\hat{k},$$

where v_r, v_θ, and w are the radial ($\hat{r}$), azimuthal ($\hat{\theta}$), and vertical ($\hat{k}$) wind components, respectively, $\boldsymbol{\omega}_H$ is the horizontal vorticity vector, and r is radius.

Here we consider only the idealized case of unidirectional azimuthal flow that increases in magnitude with height; the vertical shear vector points directly in our azimuthal direction (down azimuth) at all vertical levels. Assuming that a nascent updraft propagates roughly with the mean deep-layer azimuthal flow, the low-level (upper level) winds are slower (faster) than the propagation speed of the updraft. Thus, the updraft will receive updraft-relative inflow from the down-azimuth direction, and similarly the upper-level updraft-relative outflow will return down azimuth (Fig. 2a).

The troposphere is characterized by radially inward-directed (i.e., northward) horizontal vorticity lines that are simply a consequence of vertical shear of the azimuthal winds. Assuming that the updraft develops in an environment of negligible ambient vertical vorticity, only the first term on the right-hand side of Eq. (1) initially contributes to the vertical vorticity tendency by tilting the shear-associated horizontal vorticity lines into the vertical (Fig. 2a). Such tilting of horizontal vorticity creates locally maximized cyclonic (anticyclonic) vertical vorticity on the southern (northern) flank of the updraft—that is, to the right (left) of the vertical shear vector. Note that because the environment lacks ambient vertical vorticity, the primary updraft itself cannot acquire vertical vorticity. Wilhelmson and Klemp (1978) showed that the upward tilting of horizontal vorticity is the primary mechanism for the initial development of midlevel rotation in the supercell thunderstorm by linearizing Eq. (1) about the unidirectional azimuthal wind, yielding, in cylindrical coordinates,

$$\frac{d\zeta}{dt} = \boldsymbol{\omega}_H \cdot \nabla_H w = -\frac{\partial v_\theta}{\partial z} \cdot \frac{\partial w}{\partial r}. \tag{2}$$

As the primary updraft matures with counterrotating, tilting-generated midlevel vortices on its flanks, the midlevel rotation dynamically induces lower midlevel pressure on both flanks of the updraft (Rotunno and Klemp 1982). Subsequent updraft growth is thus favored equally within both the cyclonic- and anticyclonic-rotating members of the tilting couplet. The new rotating updrafts (one cyclonic and one anticyclonic) may each amplify the tilting-generated vorticity via stretching and begin to propagate with a component transverse to the shear vector (and coincidentally also transverse to the mean flow, which here is parallel to the shear).

Figure 3a is adapted from simulations of Weisman and Klemp (1986) and shows how a unidirectionally sheared buoyant updraft (initial 0–5-km bulk shear is $40\,\mathrm{m\,s^{-1}}$ and buoyant energy is $2200\,\mathrm{J\,kg^{-1}}$) tends to split with time. The cyclonic updraft propagates with a component to the right of the shear vector (radially outward in our coordinate framework), and the anticyclonic updraft propagates to the left of the shear vector (radially inward). Such splitting cells are commonly observed in the midlatitudes (Bluestein and Sohl 1979) and propagate as roughly a mirror image about the mean vertical shear vector (Browning 1968; Wilhelmson and Klemp 1978). In this idealized scenario, both members of the split may thrive despite their counterrotation. Observed deviant cell motion is approximately 30° from the mean flow vector

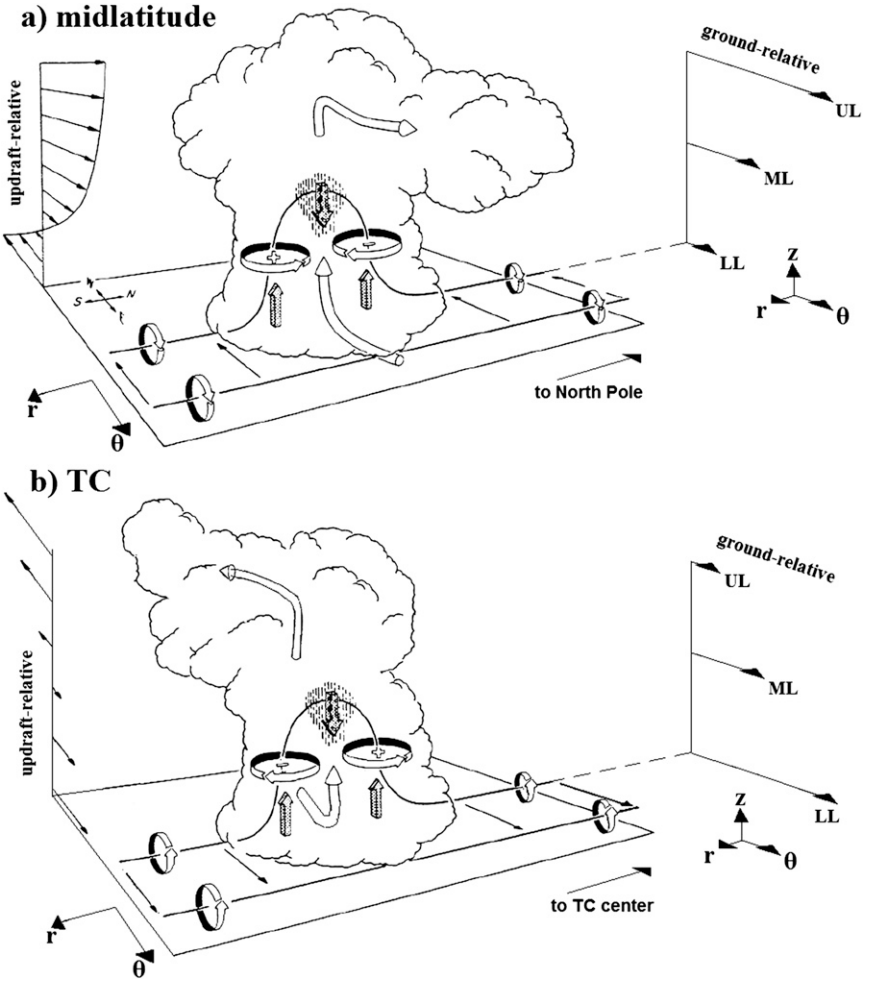

FIG. 2. Schematic depiction of an idealized updraft initiation and interaction with unidirectional vertical shear of the azimuthal winds in (a) the midlatitudes and (b) the TC. Thin solid vortex lines are encircled by flat arrows that denote the sense of rotation. Cylindrical arrows denote the updraft-relative flow, and shaded block arrows represent updrafts and downdrafts. Schematic vertical profiles of updraft (ground)-flow vectors are provided on the left (right) side of each panel. Partially adapted from Klemp (1987).

(Maddox 1976). Recent studies have developed more sophisticated methods to estimate off-hodograph updraft motion (e.g., Bunkers et al. 2000), but they are outside the scope of this study.

As the mirror-image updrafts propagate apart from one another, a component of their motion becomes orthogonal to the mean flow. This deviant motion is critical because the updraft-relative flow is no longer unidirectional, and this has implications on storm structure, evolution, and longevity. Figure 4a shows both the motion vector of each updraft and the updraft-relative flow vectors associated with each updraft. The right (left)-moving split ''feels'' an environmental flow that turns clockwise (counterclockwise) with height (see thin arrows in Fig. 4a). The low-level updraft-relative inflow into the cyclonic right-moving updraft approaches from the southeast, the midlevel updraft-relative flow is southerly, and the upper-level updraft-relative flow is southwesterly. This updraft-relative flow is consistent with the associated radar reflectivity pattern (Fig. 3a, ''RM''), which exhibits a southeast-facing inflow notch and a broad area of anvil precipitation northeast of the peak reflectivity. Because the updraft-relative flow contains a southerly component throughout the troposphere, the sharpest gradients of radar reflectivity occur on the southern, or radially outward, edge of the precipitation field where the primary updraft resides.

The anticyclonic split structure can be understood by similar comparison of the updraft-relative flow with the idealized radar-reflectivity structure. A more complete

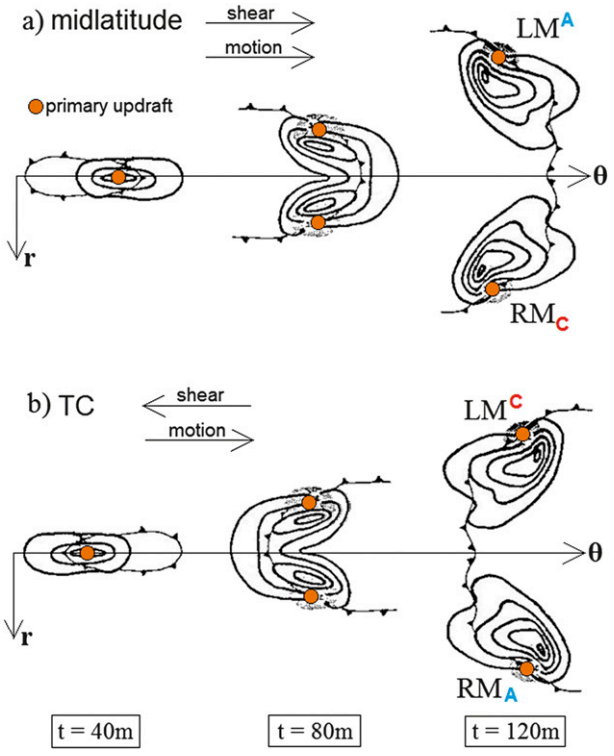

FIG. 3. Schematic plan-view depiction of a highly idealized splitting updraft in a unidirectional shear profile for (a) the midlatitudes and (b) the TC at (left) $t = 40$, (middle) $t = 80$, and (right) $t = 120$ min after updraft initiation. Left-moving (LM) and right-moving (RM) updrafts are labeled with their direction of rotation: cyclonic (C) or anticyclonic (A). Thin arrows denote the direction of vertical shear and mean wind vectors, and the thick contours represent low-level radar reflectivity. The locations of the primary midlevel updrafts are denoted by filled circles, and the boundaries of surface gust fronts are shown by cold-front symbols. Images are partially adapted from the idealized numerical simulation of Weisman and Klemp (1986, their Fig. 15.17c) and are intended here to convey only qualitative structural features. Their simulation is conducted using the cloud model of Klemp and Wilhelmson (1978) and initialized with 2200 J kg^{-1} of CAPE and 40 m s^{-1} of unidirectional westerly vertical shear.

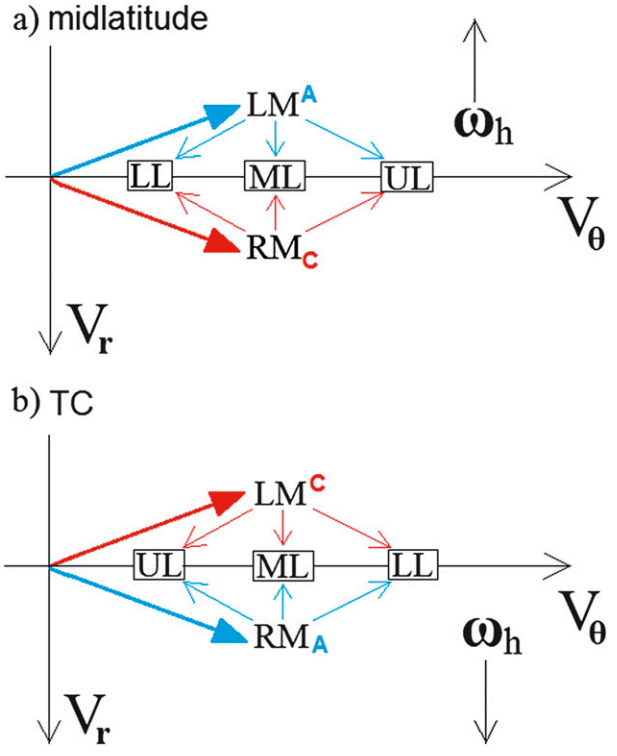

FIG. 4. Idealized hodographs showing low-level (LL), midlevel (ML), and upper-level (UL) winds for unidirectional wind profiles in (a) the midlatitudes and (b) the TC. Thick arrows denote the deviant storm-motion vector of the LM and RM members of the splitting pair. Thin arrows denote the updraft-relative wind vector at each vertical level, and "A" and "C" denote the sense of rotation of each member of the pair.

description of this classic supercell structure, including the three-dimensional airflows and implications for updraft longevity, is provided by Lemon and Doswell (1979). In section 4, we revisit other observable features of the midlatitude supercell structure within the context of the TC, including the rear-flank downdraft (RFD) and the bounded weak-echo region (BWER).

Recall that during the updraft initiation stage, the updraft-relative inflow approaches the presplit updraft from down azimuth (see Fig. 2a), exactly perpendicular to the horizontal vorticity vector. The initial updraft tilts environmental horizontal vorticity leading to the initial midlevel rotation exclusively on the flanks of the updraft, as discussed above, but the updraft itself cannot acquire rotation because the inflow contains no along-flow component of horizontal vorticity. However, once the tilting-generated vortices acquire updrafts and deviate from the mean flow, the low-level updraft-relative inflow vector for the cyclonic (anticyclonic) member of the split acquires a component that is parallel (antiparallel) to the environmental horizontal vorticity vector (Fig. 4a).

When updraft-relative inflow contains a component that is parallel (antiparallel) to the environmental horizontal vorticity vector, the flow contains streamwise (antistreamwise) vorticity (Davies-Jones 1984). Physically, streamwise (antistreamwise) inflow means that the right (left)-moving updraft may "ingest" horizontal vortex lines and create vertical vorticity via tilting that is in phase with the direction of rotation of the parent updraft. In our simple unidirectional shear example, streamwise vorticity arises solely because of the deviant storm motion (i.e., that which occurs transverse to the mean environmental wind) (Weisman and Rotunno 2000), which is a consequence of the splitting processes described above.

Cyclonically rotating updrafts that ingest streamwise horizontal vorticity immediately tilt vortex lines to create positive vertical vorticity, which then may be stretched by the updraft: a nonlinear positive feedback (the ''tilt then stretch'' mechanism) by which each updraft may quickly amplify its respective vertical vorticity.

Despite the fact that the left- and right-moving splits are equally favored for intensification in the idealized scenario, right-moving splits are far more common in the midlatitudes (Newton and Katz 1958). Previous studies (e.g., Maddox 1976) have noted that the hodograph typically turns clockwise with height in midlatitude synoptic situations that favor right-moving supercells. When the hodograph, and thus the shear vector, turn clockwise with height, the dynamically induced vertical pressure gradients tend to favor (suppress) updraft growth on the right (left)-of-shear updraft flank (Rotunno and Klemp 1982). We reserve the complication of hodograph curvature for future study, although it certainly exists in all real environments.

In summary, an updraft that forms in a unidirectionally vertically sheared environment initially acquires midlevel rotation exclusively on its flanks owing to tilting of environmental horizontal vorticity. The updraft subsequently tends to split owing to rotation-induced midlevel nonhydrostatic pressure perturbations that favor updraft growth within both rotating flanks of the original updraft. Because of continual updraft growth on the flanks of the original updraft, the counterrotating updrafts begin to propagate away from one another. The cyclonic split always deviates to the right of the shear vector, regardless of the orientation of the shear because the processes are Galilean invariant (Bunkers et al. 2000). In the midlatitudes, right (left) splits can maintain their rotation owing ingestion of low-level updraft-relative streamwise (antistreamwise) vorticity that arises because of altered updraft-relative flow. The off-hodograph propagation results in a positive feedback between low-level tilting generation and subsequent stretching in the updraft. In the midlatitudes (i.e., an environment with typically negligible ambient vertical vorticity) observations of such counterrotating mirror-image storms provided the first hint at supercell dynamics.

3. TC inner-core updrafts in vertical shear

Moving to the TC environment, we now examine TC updrafts using the same theoretical framework that has been set forth in the midlatitude literature [e.g., that summarized by Klemp (1987)]. For purposes of comparison with the case of midlatitude unidirectional shear, we retain the same cylindrical coordinate system presented above, except that the TC center is considered

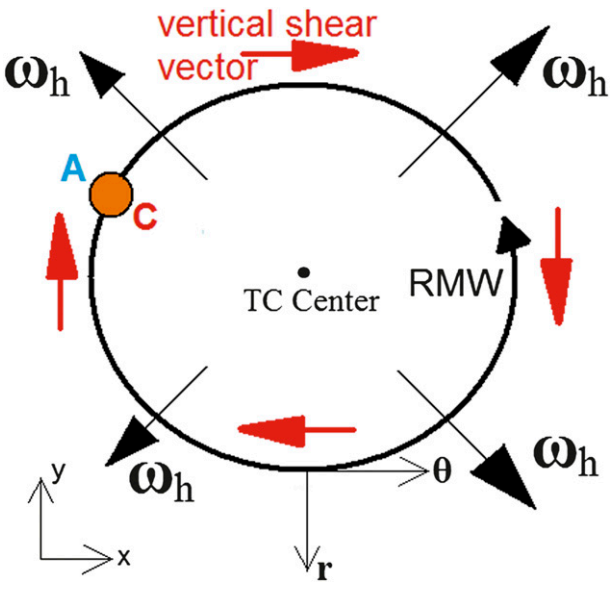

FIG. 5. Schematic depiction of the idealized TC circulation, including the outward-directed horizontal vorticity (vertical shear) vectors that are normal (antiparallel) to the azimuthal flow near the RMW. Letters ''A'' and ''C'' denote the anticyclonic and cyclonic vorticity tilting tendencies, respectively, on the flanks of an idealized initiating updraft.

the origin (Fig. 1b). Because updraft-scale convection remains the focus, Eq. (1) remains useful for our purposes. To maintain consistency with the unidirectionally sheared flow example presented in the previous section, we consider an initially axisymmetric and stationary TC vortex with purely azimuthal flow (no secondary circulation and no synoptic-scale flow).

a. Preupdraft dynamic ''environment'' and ''vertical shear''

In the midlatitude literature, the term ''environmental'' refers to a relatively uniform mesoscale environment within which the updraft develops. In the TC literature, the term environmental often refers to synoptic-scale influences on the TC-scale circulation, typically in regard to vertical shear impacts on the entire TC in a large area-averaged sense. In this section, to avoid confusion with the typical TC use of the term environmental, we instead focus only on the influences of the vortex-scale circulation locally on the updraft. The mean azimuthal vortex of the TC inner core is our ''environment'' that vertically shears updrafts that initiate within it.

If we assume that azimuthal winds peak at the ocean surface (recall that we neglect friction) and decay vertically upward, the local vertical shear vector is directed against the mean flow at all azimuths and vertical levels (Fig. 5). This shear orientation with respect to the mean flow is opposite to that discussed above for midlatitude

convection. As a consequence, $\boldsymbol{\omega}_H$ is directed 90° to the right of the mean azimuthal flow (Fig. 5)—that is, radially outward and rotated 180° from the analogous midlatitude example. In short, while the local vertical shear and mean flow vectors are parallel in the idealized midlatitude environment, they are antiparallel in the idealized TC inner core.

b. Idealized TC updraft initiation

As an updraft initiates in the TC core, we assume momentarily that it does so without any ambient vertical vorticity (obviously an invalid assumption that will be reconciled below) to demonstrate its interaction with the vortex-scale vertical shear (Fig. 2b). A nascent updraft that forms near the RMW will be sheared by the azimuthal flow, tilt downshear, and move down azimuth with the mean deep-layer azimuthal flow. Because the low-level (upper level) winds are faster (slower) than the propagation speed of the updraft, the primary updraft receives updraft-relative inflow from the up-azimuth direction, and similarly the upper-level outflow returns up azimuth (Fig. 2b).

Just as described above for midlatitude updrafts, the idealized TC updraft tilts the horizontal vorticity associated with the mean TC vortex, creating a couplet of counterrotating vertical vortices. A critical distinction between midlatitude and TC updrafts is the direction of the shear vector. Because it differs by 180° from that in Fig. 2a, and consequently so does the horizontal vorticity vector, the cyclonic member of the tilting couplet will develop radially inward, toward the TC center. This is shown schematically in Fig. 2b and has been discussed in the TC literature (e.g., Montgomery et al. 2006; Didlake and Houze 2011), although the process has not been discussed in the context of inner-core updraft propagation.

c. Idealized TC updraft maturation and "splitting"

Once the counterrotating midlevel vortices develop on the flanks of the idealized TC updraft, subsequent updraft growth is dynamically favored on both flanks because of the upward-directed nonhydrostatic pressure gradients induced by midlevel rotation (Rotunno and Klemp 1982). In theory, two counterrotating mirror-image updrafts would mature and propagate away from one another. The cyclonic member would propagate to the right of the shear vector, with a radially inward component (Fig. 3b), while the anticyclonic member would propagate to the left of the shear vector, with a radially outward component. Note that the construction of Fig. 3b consists only of rotating Fig. 3a 180° to account for the changing orientation of the shear vector.

For the moment, let us assume that TC updrafts do indeed split. At the moment of the split (i.e., the onset of off-hodograph motion), the updraft-relative inflow into each member changes, with the cyclonic (anticyclonic) member of the updraft split beginning to receive updraft-relative low-level inflow on its radially inward (outward) flank (Fig. 4b). The idealized cyclonic left split should "feel" a radially outward wind component at all levels, including low-level updraft-relative inflow on its radially inward flank. Thus, the sharpest gradients in radar reflectivity and the primary updraft should reside on the radially inward side of the heaviest precipitation (i.e., at the eye–eyewall interface), analogous to the "inflow notch" observed in midlatitude supercells. Sharp reflectivity gradients at the eye–eyewall interface, adjacent to strong updrafts located radially inward from the reflectivity maximum, have been observed in real TCs (e.g., Marks et al. 2008) and in simulated TCs (e.g., Braun et al. 2006; Houze 2010). Additionally, their upper-level outflow should occur up azimuth and partially radially outward. The conceptual model in Fig. 3b captures in plain view what these idealized left- and right-split updrafts (recall that we ignore, for now, the ambient vorticity stretched by the initial updraft) may look like on radar.

A feature of the idealized cyclonic, radially inward split is that its low-level updraft-relative inflow becomes streamwise; that is, it has a component parallel to the horizontal vorticity vector. Once the parcel reaches the updraft, it will immediately turn upward, and the horizontal vorticity is oriented such that it is instantly converted to cyclonic vertical vorticity available for stretching. Conversely, the updraft-relative inflow into the idealized anticyclonic, radially outward split is antistreamwise, and the tilting leads to instant creation of anticyclonic vertical vorticity. The tilt-then-stretch feedback will thus tend to enhance the cyclonic (anticyclonic) vorticity of the inward (outward)-propagating member of the split. Therefore, cyclonic vorticity generation and new updraft growth is perpetually favored radially inward from the location of the primary updraft initiation. Note that because the ground-relative winds are unidirectional, the idealized TC vortex contains no inherent streamwise vorticity, which arises in this scenario only when updrafts deviate from the mean flow.

Thus far we have constructed an idealized scenario that is conceptually identical to the idealized midlatitude splitting-supercell example; the shear vector orientation with respect to the mean flow is the only difference. We have ignored an obvious characteristic of the mature idealized TC vortex: it contains an abundance of ambient cyclonic vorticity, particularly in the lower troposphere where azimuthal winds are maximized, available to incipient updrafts. Because of this, recent TC updraft studies (e.g., Montgomery et al. 2006)

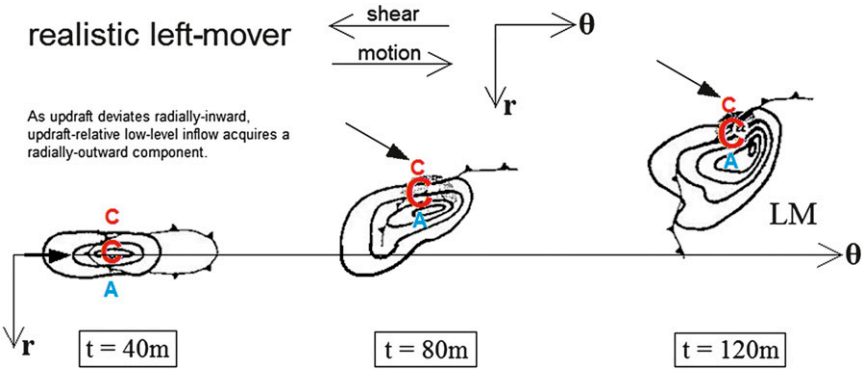

FIG. 6. As in Fig. 3, but for a more realistic TC left mover that includes the cyclonic vorticity stretching tendency (large "C," collocated with the primary updraft in all panels) likely to occur at the time of updraft initiation, and the vorticity tilting tendencies (small "A" and "C") transverse to the local shear vector. Solid arrows denote the updraft-relative low-level-flow direction.

have understandably focused primarily on stretching of ambient vorticity to explain the roles of individual updrafts in TCs. Indeed, carefully constructed vorticity budgets indicate that the stretching term is responsible for the majority of vorticity production in the low levels of the TC (Kurihara and Tuleya 1981). The distinction that we aim to make is that the tilting term may not only contribute to deviant updraft motion but also may play a role in the positive feedback between low-level tilting generation and subsequent stretching.

Now let us consider that, unlike the initial midlatitude updraft, intense TC updrafts (i.e., VHTs) do acquire low- and midlevel cyclonic rotation upon initiation owing to the stretching term in Eq. (1). Next, superimpose the tilting-generated midlevel tendencies shown in Fig. 2b. The midlevel vorticity tendencies may look something like Fig. 6 (left), with a large stretching tendency collocated with the primary VHT updraft and smaller tilting tendencies on the across-shear flanks of the VHT. In contrast to the midlatitude example, updraft growth should be favored both within the original rotating VHT that is constantly stretching ambient vertical vorticity and on the flanks where midlevel tilting-generated vertical vorticity promotes new updraft growth.

However, the tilting-generated midlevel tendencies should play a slightly different role than that which leads to updraft splitting in the midlatitudes. The cyclonic (anticyclonic) member of the tilting tendency pair will simply act to enhance (suppress) updraft growth on the radially inward (outward) flank of the VHT. In other words, the anticyclonic tilting tendency may not be of sufficient magnitude to generate a distinct anticyclonically rotating, right-moving updraft as suggested in Fig. 3b, given the richly vortical environment of the TC core. Instead, the superposition of tilting and stretching tendencies may lead to a radially inward bias of the primary updraft (Fig. 6, middle) and, consequently, a radially inward deviant motion of the VHT. As it deviates radially inward, it ingests low-level streamwise vorticity, further enhancing the cyclonic vorticity of the initial VHT via the nonlinear tilt-then-stretch feedback set forth above. Hereafter, we refer to this highly idealized, mature cyclonic VHT (Fig. 6, right) as a "left mover."

Anticyclonic VHTs, or "right movers," which theoretically propagate with a radially outward component and ingest antistreamwise horizontal vorticity (Fig. 3b), are probably rare given the richly cyclonic vortical TC environment. Regardless, the suppression of cyclonic vorticity associated with the radially outward anticyclonic tilting tendency may impact the radially outward flank of the left mover. If this process is active in real TCs, when the anticyclonic tendency is large enough to strongly suppress the upward motion on the radially outward flank of the left-mover updraft, it may be helpful to understand the generation of a moat region between the eyewall and the outer rainbands.

d. "Left movers" as eyewall contractors

If stretching of ambient cyclonic vorticity alone were responsible for the evolution of all VHTs, one may not expect a unique radar reflectivity structure other than the shearing associated with the vertical shear of the azimuthal winds (Fig. 2b). However, when an updraft deviates from the mean flow, the altered updraft-relative flow suggests that a more complex precipitation structure may evolve (Fig. 6). For example, the primary updraft and the sharpest reflectivity gradients should occur radially inward from the heaviest precipitation (Fig. 6, right).

Theoretically, these ''left movers'' (with regard to the mean TC azimuthal flow) could play a dramatic role in TC evolution. Analogous to their midlatitude right-moving supercell counterparts, they comprise a single dominant rotating updraft that constantly ingests streamwise vorticity on its radially inward flank and propagates partially toward its right-of-shear flank (i.e., toward the TC center). The left movers may generate considerable vertical vorticity due to the nonlinear tilt-then-stretch mechanism. In this sense, they convert horizontal vorticity from the vertical shear of the mean vortex into vertical vorticity and transport it inward toward the TC center. If it occurs in real TCs, this process may play some role in the observed tendency of convective eyewalls, and thus RMWs, to contract.

The mechanism is quite distinct to the symmetric mechanisms proposed by Shapiro and Willoughby (1982) and the asymmetric mixing process presented by Schubert et al. (1999). Specifically, the left-mover hypothesis suggests an active role for updraft-scale convection without invoking the secondary TC circulation, which plays a central role in the eyewall contraction theory of Shapiro and Willoughby (1982). Additionally, it could be helpful in understanding why cyclonic vorticity tends to congregate near the center of intensifying warm-core disturbances (Montgomery et al. 2006) and why intensifying TCs often exhibit intense updrafts inside the RMW (Vigh and Schubert 2009) in larger proportion than mature TCs (Rogers et al. 2013).

4. Evidence of left movers and their local environment

In the midlatitudes, 0–6-km bulk vertical shear is greater than $10\,\mathrm{m\,s^{-1}}$ in the vast majority of supercell cases (Bunkers 2002). Aside from the necessary shear (and the necessity of positive buoyancy), other studies find that supercells can occur in a wide spectrum of shear and instability environments (Weisman and Klemp 1982; Rasmussen and Blanchard 1998). We do not speculate on the direct applicability of midlatitude results to the TC core, but it is certainly possible that the peak tangential wind near the top of the hurricane boundary layer (HBL) $V_{\max}$ may decay at a similar rate in the lowest 6 km above the level of $V_{\max}$. We exclude the HBL here to focus on the interaction of deep, buoyant updrafts that are often maximized in the midlevels (Braun 2002; Rogers 2010) with the deep-layer vertical shear. Although most of the updraft is contained within this deep layer, the strongly sheared HBL is a critical complexity for future study.

Radar analyses by Reasor et al. (2009) show an azimuthal-mean tangential wind decay of about $12\,\mathrm{m\,s^{-1}}$ in the 1–7-km layer (their Fig. 10a) within an intensifying TC. Observational analyses by Stern and Nolan (2011) show roughly a $10\,\mathrm{m\,s^{-1}}$ decay of the maximum tangential winds in the 2–8-km layer (their Fig. 1) for a range of TC cases and intensities. In comparison to midlatitude supercell environments, the vertical shear of the TC azimuthal winds is likely lower. Certainly the shear magnitude and decay with height varies spatially, particularly in synoptically sheared TCs.

In Fig. 7 the airborne Doppler radar–observed (Gamache 1997) local vertical shear during the RI of Hurricane Earl (2010) is shown. During the 30-h period shown in Fig. 7 (0600 UTC 29 August–1200 UTC 30 August), Earl intensified by 50 knots (kt; $1\,\mathrm{kt} = 0.51\,\mathrm{m\,s^{-1}}$) from 55 to 105 kt. At the beginning of the RI process (Fig. 7a), local vertical shear near the center of circulation exhibits an anticyclonic pattern, as expected in any vortex where tangential winds decay with height (see Fig. 5). The 1–7-km bulk shear magnitudes are generally less than $15\,\mathrm{m\,s^{-1}}$ near and within the RMW. When Earl reaches hurricane status (Fig. 7b), the anticyclonic shear pattern appears more symmetric and notably stronger, with local magnitudes exceeding $15\,\mathrm{m\,s^{-1}}$ around nearly the entire circumference of the center, including near and within the RMW. The shear structure observed in Fig. 7b during RI is quite similar to that conceptualized in the previous section in that the local shear vector generally opposes the mean cyclonic flow.

A coincident airborne radar image in Fig. 8a depicts several updraft-scale convective features that resemble the idealized left mover and occur in the southeastern quadrant where local shear exceeds $15\,\mathrm{m\,s^{-1}}$. Although the radar data were not sufficient to determine updraft motion with respect to the mean flow, structural characteristics including sharp radially inward reflectivity gradients may imply movement that is left of the mean flow. It is important to note that inward updraft propagation is not the only reason why sharp reflectivity gradients may exist, as the TC eye is characterized by generally dry, subsiding air.

Figures 8b–d show three additional cases of TCs undergoing RI; all data were acquired during the period of most rapid intensification, as indicated by the National Hurricane Center best-track dataset (Jarvinen et al. 1984; McAdie et al. 2009). All of the TCs exhibit at least one distinct convective feature with structural characteristics of the idealized left mover. The approximate locations of possible left movers are denoted by crosses in Fig. 8. Of interest is that the convective features are not isolated, as midlatitude supercells often are, likely because they are superimposed on the general mesoscale ascent of the TC inner core (Eastin et al. 2005).

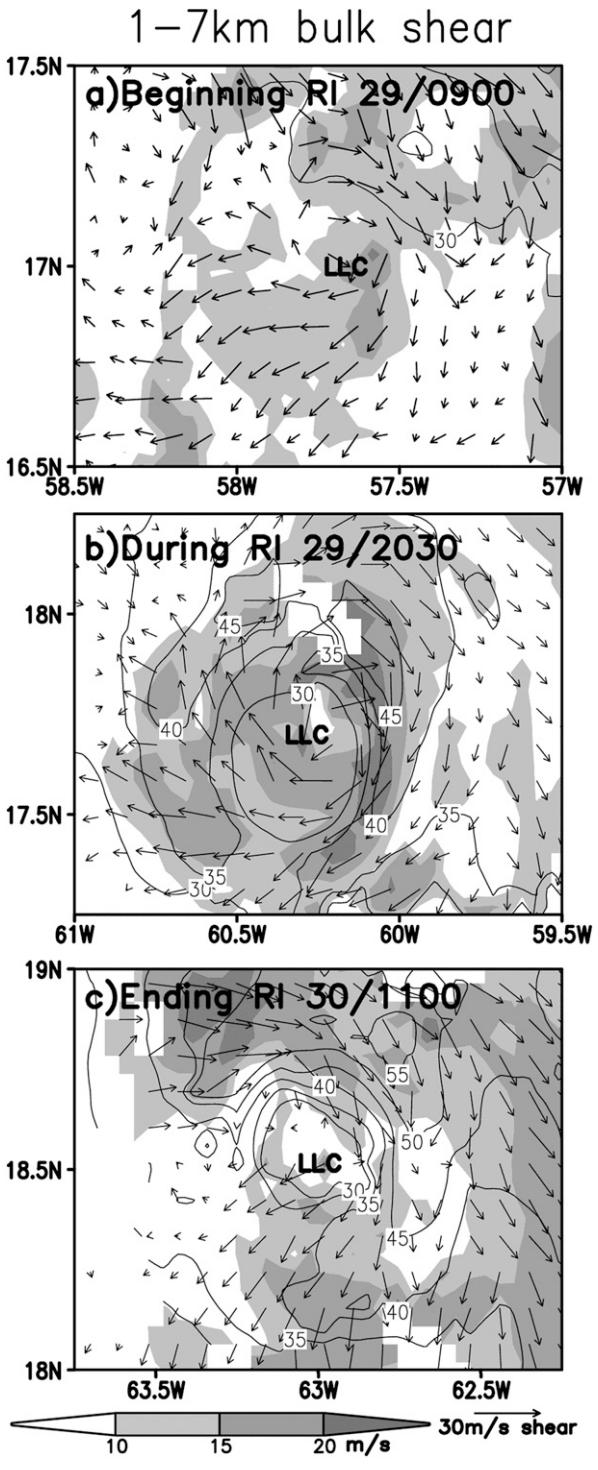

FIG. 7. The 1–7-km bulk vertical wind shear vectors and magnitude (shaded, $m\,s^{-1}$) and 1-km horizontal wind speed (contoured with a $5\,m\,s^{-1}$ interval) calculated from tail Doppler radar composites obtained for three flights at the (a) beginning, (b) middle, and (c) ending stages of the RI of Hurricane Earl (2010). The low-level (1 km) center of circulation (LLC) and the approximate time of the first flight leg of data acquisition are noted in each panel. Data courtesy of the NOAA Hurricane Research Division (HRD) of Atlantic Oceanographic and Meteorological Laboratory (AOML) (NOAA/AOML/HRD).

As Earl became a major hurricane (Fig. 7c), the inner-core shear pattern still exhibited some anticyclonic curvature, but the magnitudes inside the RMW diminished to generally less than $15\,m\,s^{-1}$, despite the fact that Earl had become a major hurricane and developed a satellite-observed eye (not shown). The diminished shear suggests that during the early stages of RI the low-level winds increased more quickly than the midlevel winds, effectively enhancing the local vertical shear. Subsequent intensification likely occurred more quickly in the midlevels as the vortex deepened, effectively diminishing the local shear. In short, 1–7-km bulk vertical shear magnitudes of $15\,m\,s^{-1}$ may have been sufficient to support left movers, although herein we address neither the shear thresholds nor the thermodynamic thresholds that are necessary. Complete analysis of this topic must consider total vertical shear (i.e., the total length of the hodograph), including the strongly sheared HBL that we ignore here for simplicity.

In a study of the intensification of the strongly sheared Tropical Storm Gabrielle (2001), Molinari and Vollaro (2010, hereafter MV10) investigated the characteristics of an intense convective cell in the northern portion of the circulation using ground-based radar. Their westerly sheared synoptic-scale environment differs dramatically from the idealized quiescent environment described above. They tracked cloud-to-ground lightning strikes (Fig. 9a herein), presumably associated with the primary updraft(s) within the distinct cell. They found that the cyclonically rotating cell moved cyclonically and radially inward.

The reflectivity structure of the cell (Fig. 9a, inset) is similar to the theoretical left mover described previously in this section (cf. Figs. 9a and 6), with an inflow notch and sharp reflectivity gradients on the radially inner edge and broad area of anvil precipitation radially outward and up azimuth from the cell. The radar algorithm identified the primary rotating updraft as a mesocyclone (e.g., Stewart and Lyons 1996), which occurred in the expected location (Fig. 6, right) on the radially inner edge and down azimuth from the majority of the reflectivity field. This reflectivity structure suggests radially outward updraft-relative flow at the height of the beam (0.5° tilt) and may imply movement to the left of the mean flow.

Although somewhat outside the scope of this study, it is noteworthy that a south–north-oriented gust front, possibly associated with the leading edge of an RFD (van Tassel 1955; Markowski 2002), is apparent radially inward from the highest reflectivity (cf. Fig. 9a, inset, and Fig. 6). The RFD is so named because it occurs on the trailing upstream flank of a midlatitude supercell. However, since the structure of the left mover is distinct from the midlatitude supercell, the RFD-like feature occurs on the leading downstream flank (see Fig. 6, right).

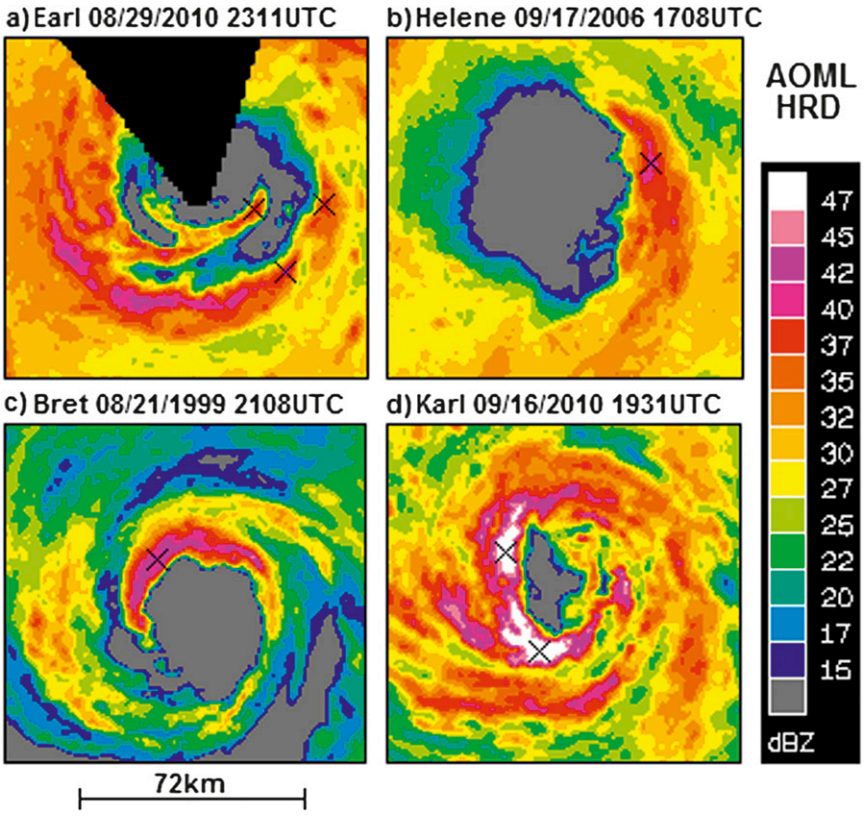

FIG. 8. Radar reflectivity (shaded, dB*Z*) acquired by the lower-fuselage radar aboard a NOAA P-3 aircraft during RI of Hurricanes (a) Earl, (b) Bret, (c) Helene, and (d) Karl. Data in (a) was acquired during the third of the four flight legs used to create the composite structure in Fig. 7b, and data are unavailable in the removed wedge. Flight altitude was approximately 2000 (4000) m in Helene and Earl (Bret and Karl), and the aircraft was located within the eye in all four cases. 24-h intensity changes, centered on the nearest synoptic time for (a)–(d) are 40, 30, 45, and 50 kt, respectively. Note that the reflectivity legend applies directly to (a) and (d), but the range in (b) and (c) are 20–52 and 20–47 dB*Z*, respectively. Crosses denote the precipitating region of possible left movers. Data courtesy of NOAA/AOML/HRD.

For comparison with the MV10 convective cell, Figs. 10a and 10b show the low-level structure of a smaller but similar feature from the simulation of Hogsett and Zhang (2010) of an intensifying TC. The cell developed in the northern portion of the developing circulation and exhibited many similar features to the MV10 study, including an updraft collocated with the mesocyclone and sharp reflectivity gradients where the low-level inflow enters the updraft (Fig. 10a). The low-level vorticity tendencies (Fig. 10b) show evidence of positive-tilting generation occurring within the inflow and subsequent stretching in the updraft. Several such rotating updrafts developed and moved cyclonically and inward (not shown) as the TC intensified. Although the HBL processes shown in Fig. 10 are not fully investigated herein, they must be investigated further to completely understand the behavior of these features in real TCs.

MV10 concluded that "in the high-vorticity environment within the core of a hurricane, only right-moving supercells would be expected," and in part because this cell did not move to the right of the mean wind, they placed it within the more general category of a VHT. Based on the arguments herein and those emphasized in Bunkers et al. (2000), it is not the propagation with respect to the mean wind that is important, but rather the fact that it may have moved to the right of the local vertical shear vector. In the TC inner core above the HBL, right of shear is toward the left of the mean wind, cyclonically, and inward.

Reasor et al. (2009) and Sitkowski and Barnes (2009) have reported on similar "inward spiraling" of eyewall convection within rapidly intensifying (and also moderately environmentally sheared) Hurricane Guillermo (1997). Sitkowski and Barnes (2009) concluded that mixing between the eye and eyewall likely led to the reduction in eye diameter, but we suggest that convective

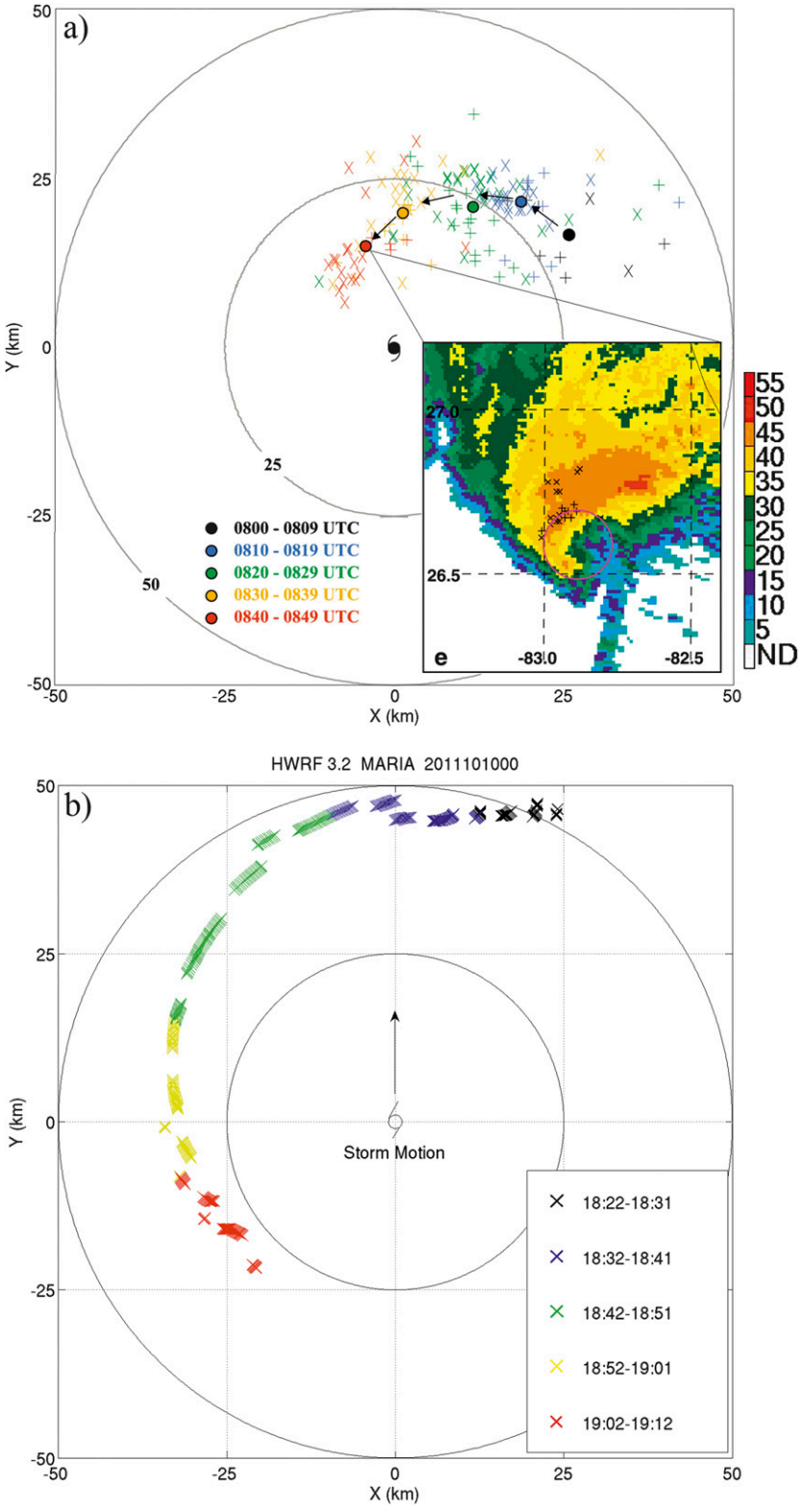

FIG. 9. (a) Storm-center-relative cloud-to-ground lightning strikes associated with the evolution of the inset convection north of the center of Tropical Storm (TS) Gabrielle (2001) on 14 Sep [adapted from MV10 (their Figs. 5 and 6e)]. (b) The location of storm-center-relative maximum wind from a semioperational HWRF model forecast of TS Maria (2011). Note the cyclonic and radially inward propagation in (a) and (b).

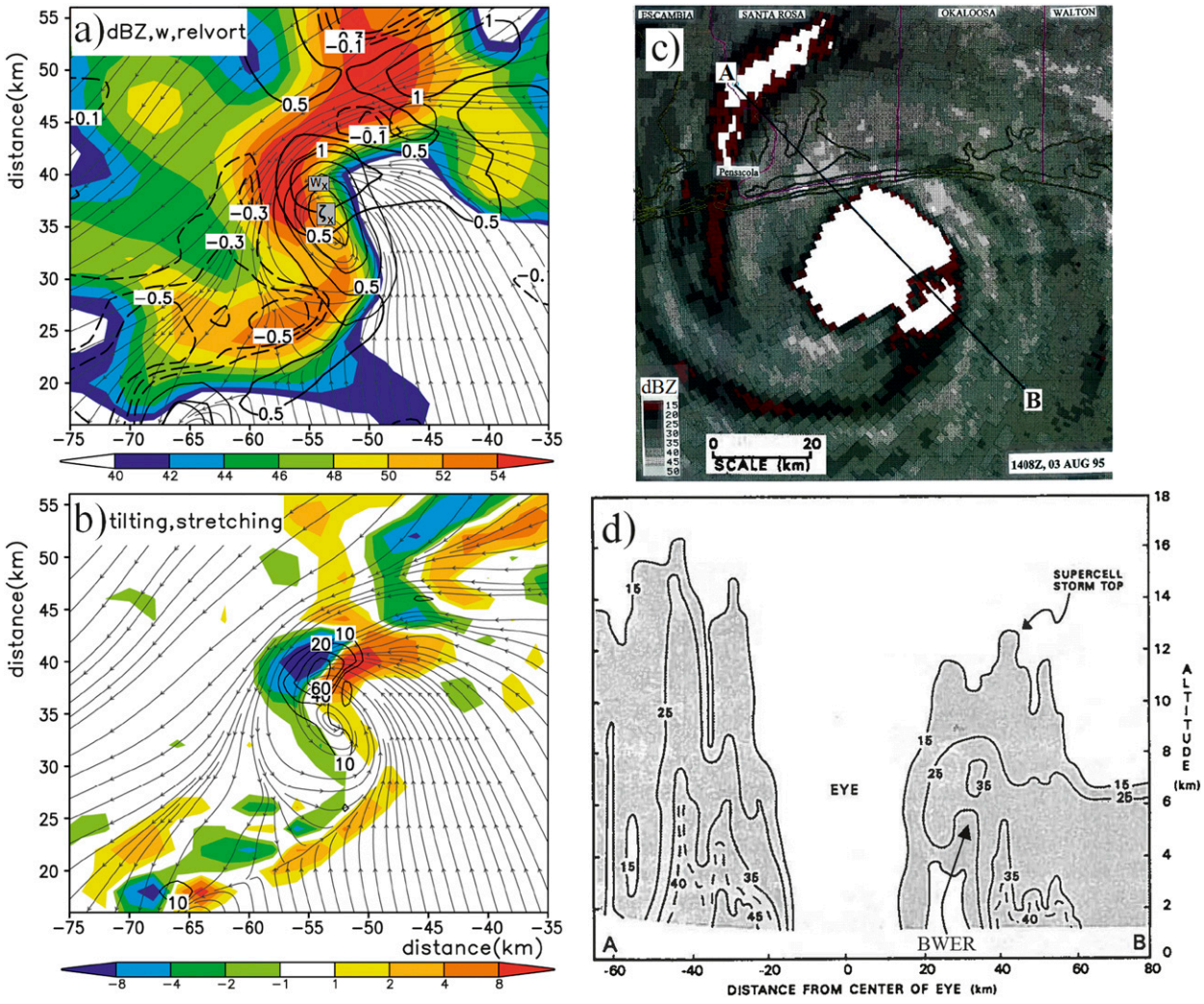

FIG. 10. (left) A 2-km WRF-simulated updraft, including 950-hPa (a) radar reflectivity (shaded, dBZ), vertical motion (thick contours, m s^{-1}; w_x denotes local maximum), and relative vorticity (light contours at 2, 4, 6, 8, and 10×10^{-3} s^{-1}; ζ_x denotes local maximum), and (b) tilting rates (shaded, $\times 10^{-6}$ s^{-2}) and stretching rates (contours, $\times 10^{-6}$ s^{-2}). The updraft is located approximately 50 km north-northwest of the low-level pressure center of an intensifying TC, as simulated by Hogsett and Zhang (2010). Streamlines at 950 hPa are superposed, and note that the shading in (a) excludes reflectivity below 40 dBZ. (right) Ground-based radar (Eglin Air Force Base, KEVX) reflectivity of Hurricane Erin (1995) at 1408 UTC 3 Aug 1995: (c) horizontal and (d) vertical cross sections [adapted from Stewart et al. (1997, their Figs. 2 and 3)]. Reflectivity is shaded in (c) and hand contoured in (d) at 5-dBZ intervals above 15 dBZ. The northwest–southeast transect in (c) is depicted by the line segment AB.

elements may play a more active role in facilitating the contraction by propagating left of the mean azimuthal flow. Additionally, Willoughby (1998) hypothesized that during intensification low-level moist air in the eye may be drawn radially outward into the eyewall, presumably by deep convective elements within the eyewall, and Stewart et al. (1997) hypothesized that vigorous updrafts associated with long-lived eyewall supercells could more rapidly transport mass out of the base of the eye than can occur through typical eyewall diffusion processes. These hypotheses are consistent with the radially outward updraft-relative low-level inflow into the left mover (Fig. 6) and suggest a possible connection between the left mover and TC intensification.

Using the plotting convention of MV10, Fig. 9b shows an indirect example of a left-moving cell within the core of a simulated intensifying TC. This example is acquired from an experimental version of the 2011 National Oceanic and Atmospheric Administration (NOAA) Hurricane Weather Research and Forecasting (HWRF) model run at 3-km horizontal resolution and shows the location of maximum low-level wind, which is associated with a distinct convective region (not shown) during a time period of similar duration to that shown in Fig. 9a.

Within a period of less than 1 h, the location of maximum wind is shown to move radially inward from approximately 50 to 25 km. The presence of this inward-moving feature coincides with the first few hours of simulated RI and is associated with a general decrease in the RMW.

As a final example to clarify some of the structural characteristics of left movers, we show in Figs. 10c and 10d the radar depiction of an intense cell within Hurricane Erin (1995). Intense midlatitude supercells often exhibit a structure in the vertical reflectivity profile known as a BWER (Chisholm and Renick 1972) that is collocated with the primary updraft, around which hydrometeors fall and above which large hydrometeors may be suspended. Thus the BWER is a relatively low-reflectivity region that extends upward into the midtroposphere and is horizontally (and vertically above) surrounded by higher reflectivities. Figure 10d shows a radar-observed eyewall BWER extending up to almost 6 km that was analyzed by Stewart et al. (1997). We emphasize the BWER because it indicates the location of an intense updraft, which in this case is located radially inward from the maximum reflectivity. And although outside the scope of this study, a hooklike feature is apparent in the southeastern quadrant of the eye (Fig. 10c) and is consistent with the proposed left-mover structure.

The horizontal reflectivity structure shown by Stewart et al. (1997) differs somewhat from the conceptual model presented in Fig. 6 in that a distinct left mover is not easily distinguishable from the other elements of the eyewall. This is likely a frequent occurrence in the mature TC eyewall, where several left movers may coexist in close proximity and shroud the precipitation structure of neighboring cells (see Fig. 8d). Additionally, not all precipitation processes in the TC inner core are directly related to intense deep updrafts, which constitute a very small percentage of the eyewall area (Braun 2002), even though the entire eyewall may be characterized by high radar reflectivity. Essentially, the buoyant updrafts are superimposed on mesoscale ascent (Eastin et al. 2005).

5. Discussion and forecasting implications

In this study, we have shown that a highly idealized TC vortex in a quiescent synoptic environment, without regard for the TC secondary circulation, may support left-moving cyclonically rotating convective updrafts, or ''left movers.'' Similar to midlatitude cyclonic supercells, they propagate to the right of the local shear vector, which coincidentally is to the left of the mean azimuthal flow in the TC inner core.

We hypothesize that the dynamics responsible for the left-mover evolution is identical to that which causes midlatitude supercells to deviate from their mean flow: tilting of the horizontal vorticity associated with vertical shear of the deep-layer azimuthal flow. In the case of the TC, the vertical shear is an inherent feature of the warm-core vortex, in which azimuthal winds decay with height above the HBL. Left movers propagate with a radially inward component and may help to understand the cyclonic vorticity congregation and eyewall contraction that occur within intensifying TCs.

We propose that left movers are a unique class of mature VHTs, which, analogous to midlatitude supercells, may be favored in the vertically sheared local environment near the TC RMW. We suggest that VHTs of the type presented by Montgomery et al. (2006) are more general TC convective features that rely primarily on stretching ambient vorticity. If the updrafts develop with sufficient vortex-scale vertical shear (distinct from the often-considered synoptic environmental vertical shear) near the RMW, they may evolve into the left mover conceptualized in Fig. 6 and invoke a more complex dynamical process involving the feedback between tilting and stretching.

We must emphasize our critical assumption of unidirectional shear. Unlike in the midlatitudes, the vertical shear vector in a real TC likely reverses direction near the top of the HBL. Thus, the local shear vector is likely directed inward, not outward as we assume, in the lowest kilometer when friction is considered. We simplify the analysis herein to understand the propagation of deep updrafts associated with perpetual midlevel tilting on their flanks. However, ignoring the HBL certainly has implications on the low-level inflow into the proposed left mover: How can a real left mover ingest low-level streamwise vorticity on its radially inward side, as proposed, when radial inflow in a real TC originates primarily outside the eyewall? We do not aim to completely answer this question, but we point out that Braun (2002) and Houze (2010) discuss how low-level parcels actually penetrate into the eye before returning radially outward into intense eyewall updrafts. In addition to gaining buoyancy through entrainment of moist low-level eye air, this process may help to explain how left movers receive inflow on their radially inward flank. Undoubtedly, many questions remain, and this study represents only one step toward understanding such intense updrafts occurring within the TC core.

We have shown evidence from an array of sources that suggests such features may actually occur within intensifying TCs, but more work is required owing to a number of assumptions made in this study. A semantic point that we emphasize is that it may be misleading to describe such a discrete buoyant TC updraft as a supercell. Supercells have a long history in the literature as

a midlatitude and TC rainband phenomenon, and much of the discourse on their behavior contains implicit assumptions not applicable to the TC. One such assumption is that the supercell is a right-moving phenomenon with respect to the mean wind. While this is nearly always true in the midlatitudes where the vertical shear and mean wind are often parallel to first order, it is false in the typical TC inner core where the local vertical shear and mean flow above the HBL are antiparallel.

For the same reasons that midlatitude supercells exhibit longevity compared to generic updrafts that develop in low-shear environments, including updraft–downdraft separation, left movers may be longer lived than generic VHTs and more efficient at producing vorticity by first converting it from the preexisting vertically sheared flow and subsequently stretching it. This tilt-then-stretch nonlinear feedback may help to understand the connection between inner-core deep convection and RI. Specifically, left movers rapidly generate vorticity and transport it radially inward, and they may be capable of rapidly removing mass from the low-level TC eye.

Unlike their midlatitude supercell counterparts that form in relatively uniform mesoscale environments, left movers are likely confined to the comparatively small region near the RMW and occur when and where the vertical shear of the azimuthal flow is sufficient. It is certainly possible that the miniature supercells known to occur in the outer TC rainbands (Novlan and Gray 1974; McCaul 1991; Eastin and Link 2009) may share some similarities with both left movers and midlatitude supercells. Midlatitude supercells are often very long lived, partly because they develop in a comparatively uniform environment. Because of the confined local environment in which left movers evolve, they may exit the favorable area as they deviate radially inward. This suggests relatively shorter life spans of left movers compared to midlatitude supercells.

Given the idealized environment conceptualized here, left movers are internal features of the TC vortex. Left movers do not require ambient streamwise vorticity in the local environment, as even unidirectionally sheared azimuthal flow may be sufficient to cause off-hodograph updraft motion. However, as the results of MV10 imply, left movers may occur in synoptically sheared TCs also. The superposition of synoptic complexities and hodograph curvature (including the HBL) onto the idealized vortex presented herein remains a topic for future study.

From a forecasting point of view, the results of this study have some important implications. First and not surprisingly, updraft-scale dynamics, including nonhydrostatic and nonlinear dynamics, may be critical to TC evolution. To realistically capture these processes and the feedbacks on the vortex scale, numerical models must adequately represent an updraft from initiation to decay and capture structural nuances including updraft tilt and updraft–downdraft separation. Additionally, the size of the simulated updraft may be critical, since an overestimate of the updraft size may lead to an overestimate of the nonlinear tilt-then-stretch processes and thus an overforecast of vorticity generation and possibly TC intensity. Thus, the finest possible model grid spacing is desirable to fully resolve individual updrafts. From a data acquisition perspective, the vertical profile of azimuthal winds in the eyewall may be critical. Airborne Doppler radars are best suited to acquire such comprehensive data at present.

Whether the dynamics of these proposed left movers are in fact analogous to midlatitude supercells, as we argue herein, requires much continued research because of significantly differing thermodynamic, vertical shear, and instability profiles and differing spatial variability of the local vertical shear, preexisting ambient vorticity in the TC core, differing microphysical characteristics, etc., between the two environments. Perhaps most important for future study is the role of the HBL, because unlike in the midlatitudes, the local vertical shear vector in the TC inner core reverses direction near the top of the HBL.

Acknowledgments. We thank Chris Landsea and David Zelinsky of NHC for helpful reviews of the manuscript and assistance constructing several figures, as well as the HWRF teams at both the National Centers for Environmental Prediction (NCEP) Environmental Modeling Center (EMC) and the Hurricane Research Division (HRD) for providing very high temporal-resolution data from the HWRF model. The provocative comments of three anonymous reviewers significantly improved the manuscript. Airborne radar data were provided courtesy of the NOAA Hurricane Research Division of AOML in Miami, Florida. This work was supported by the NOAA Hurricane Forecast Improvement Program (HFIP).

REFERENCES

Black, M. L., and H. E. Willoughby, 1992: The concentric eyewall cycle of Hurricane Gilbert. *Mon. Wea. Rev.,* **120,** 947–957.

——, R. W. Burpee, and F. D. Marks Jr., 1996: Vertical motion characteristics of tropical cyclones determined with airborne Doppler radial velocities. *J. Atmos. Sci.,* **53,** 1887–1909.

Bluestein, H. B., and C. J. Sohl, 1979: Some observations of a splitting severe thunderstorm. *Mon. Wea. Rev.,* **107,** 861–873.

Braun, S. A., 2002: A cloud-resolving simulation of Hurricane Bob (1991): Storm structure and eyewall buoyancy. *Mon. Wea. Rev.,* **130,** 1573–1592.

——, M. T. Montgomery, and Z. Pu, 2006: High-resolution simulation of Hurricane Bonnie (1998). Part I: The organization of eyewall vertical motion. *J. Atmos. Sci.,* **63,** 19–42.

Browning, K. A., 1968: The organization of severe local storms. *Weather,* **23,** 429–434.

Bunkers, M. J., 2002: Vertical wind shear associated with left-moving supercells. *Wea. Forecasting,* **17,** 845–855.

——, B. A. Klimowski, J. W. Zeitler, R. L. Thompson, and M. L. Weisman, 2000: Predicting supercell motion using a new hodograph technique. *Wea. Forecasting,* **15,** 61–79.

Cangialosi, J. P., and J. L. Franklin, 2011: 2010 National Hurricane Center forecast verification report. NHC Forecast Verification Rep., 77 pp. [Available online at http://www.nhc.noaa.gov/verification/pdfs/Verification_2010.pdf.]

Chen, H., D.-L. Zhang, J. Carton, and R. Atlas, 2011: On the rapid intensification of Hurricane Wilma (2005). Part I: Model prediction and structural changes. *Wea. Forecasting,* **26,** 885–901.

Chisholm, A. J., and J. H. Renick, 1972: The kinematics of multicell and supercell Alberta hailstorms. Research Council of Alberta Hail Studies Rep. 72-2, 24–31.

Corbosiero, K. L., J. Molinari, and M. L. Black, 2005: The structure and evolution of Hurricane Elena (1985). Part I: Symmetric intensification. *Mon. Wea. Rev.,* **133,** 2905–2921.

Davies-Jones, R., 1984: Streamwise vorticity: The origin of updraft rotation in supercell storms. *J. Atmos. Sci.,* **41,** 2991–3006.

Didlake, A. C., and R. A. Houze, 2011: Kinematics of the secondary eyewall observed in Hurricane Rita (2005). *J. Atmos. Sci.,* **68,** 1620–1636.

Eastin, M. D., and M. C. Link, 2009: Miniature supercells in an offshore outer rainband of Hurricane Ivan (2004). *Mon. Wea. Rev.,* **137,** 2081–2104.

——, W. M. Gray, and P. G. Black, 2005: Buoyancy of convective vertical motions in the inner core of intense hurricanes. Part I: General statistics. *Mon. Wea. Rev.,* **133,** 188–208.

Gamache, J. F., 1997: Evaluation of a fully three-dimensional variational Doppler analysis technique. Preprints, *28th Conf. on Radar Meteorology,* Austin, TX, Amer. Meteor. Soc., 422–423.

Guimond, S. R., G. M. Heymsfield, and F. J. Turk, 2010: Multiscale observations of Hurricane Dennis (2005): The effects of hot towers on rapid intensification. *J. Atmos. Sci.,* **67,** 633–654.

Hack, J. J., and W. H. Schubert, 1986: Nonlinear response of atmospheric vortices to heating by organized cumulus convection. *J. Atmos. Sci.,* **43,** 1559–1573.

Hendricks, E. A., M. T. Montgomery, and C. A. Davis, 2004: The role of ''vortical'' hot towers in the formation of Tropical Cyclone Diana (1984). *J. Atmos. Sci.,* **61,** 1209–1232.

Hogsett, W., and D.-L. Zhang, 2010: Genesis of Typhoon Chanchu (2006) from a westerly wind burst associated with the MJO. Part I: Evolution of a vertically tilted precursor vortex. *J. Atmos. Sci.,* **67,** 3774–3792.

Houze, R. A., Jr., 2010: Clouds in tropical cyclones. *Mon. Wea. Rev.,* **138,** 293–344.

Jarvinen, B. R., C. J. Neumann, and M. A. S. Davis, 1984: A tropical cyclone data tape for the North Atlantic basin, 1886–1983: Contents, limitations, and uses. NOAA Tech. Memo. NWS NHC 22, 21 pp.

Klemp, J. B., 1987: Dynamics of tornadic thunderstorms. *Annu. Rev. Fluid Mech.,* **19,** 369–402.

——, and R. B. Wilhelmson, 1978: The simulation of three-dimensional convective storm dynamics. *J. Atmos. Sci.,* **35,** 1070–1096.

Kurihara, Y., and R. E. Tuleya, 1981: A numerical simulation study on the genesis of a tropical storm. *Mon. Wea. Rev.,* **109,** 1629–1653.

Lemon, L. R., and C. A. Doswell, 1979: Severe thunderstorm evolution and mesocyclone structure as related to tornadogenesis. *Mon. Wea. Rev.,* **107,** 1184–1197.

Liu, Y., D.-L. Zhang, and M. K. Yau, 1999: A multiscale numerical study of Hurricane Andrew (1992). Part II: Kinematics and inner-core structures. *Mon. Wea. Rev.,* **127,** 2597–2616.

Maddox, R. A., 1976: An evaluation of tornado proximity wind and stability data. *Mon. Wea. Rev.,* **104,** 133–142.

Markowski, P. M., 2002: Hook echoes and rear-flank downdrafts: A review. *Mon. Wea. Rev.,* **130,** 852–876.

Marks, F. D., P. G. Black, M. T. Montgomery, and R. W. Burpee, 2008: Structure of the eye and eyewall of Hurricane Hugo (1989). *Mon. Wea. Rev.,* **136,** 1237–1259.

McAdie, C. J., C. W. Landsea, C. J. Neumann, J. E. David, E. S. Blake, and G. R. Hammer, 2009: Tropical cyclones of the North Atlantic Ocean, 1851-2006. National Climatic Data Center Historical Climatology Series 6-2, 238 pp.

McCaul, E. W., Jr., 1991: Buoyancy and shear characteristics of hurricane–tornado environments. *Mon. Wea. Rev.,* **119,** 1954–1978.

——, and M. L. Weisman, 1996: Simulation of shallow supercell storms in landfalling hurricane environments. *Mon. Wea. Rev.,* **124,** 408–429.

Molinari, J., and D. Vollaro, 2010: Rapid intensification of a sheared tropical storm. *Mon. Wea. Rev.,* **138,** 3869–3885.

Monette, S. A., C. S. Velden, K. S. Griffin, and C. M. Rozoff, 2012: Examining trends in satellite-detected tropical overshooting tops as a potential predictor of tropical cyclone rapid intensification. *J. Appl. Meteor. Climatol.,* **51,** 1917–1930.

Montgomery, M. T., M. E. Nicholls, T. A. Cram, and A. B. Saunders, 2006: A vortical hot tower route to tropical cyclogenesis. *J. Atmos. Sci.,* **63,** 355–386.

Newton, C. W., and S. Katz, 1958: Movement of large convective rainstorms in relation to winds aloft. *Bull. Amer. Meteor. Soc.,* **39,** 129–136.

Novlan, D. J., and W. M. Gray, 1974: Hurricane-spawned tornadoes. *Mon. Wea. Rev.,* **102,** 476–488.

Rappaport, E. N., and Coauthors, 2009: Advances and challenges at the National Hurricane Center. *Wea. Forecasting,* **24,** 395–419.

Rasmussen, E. N., and D. O. Blanchard, 1998: A baseline climatology of sounding-derived supercell and tornado forecast parameters. *Wea. Forecasting,* **13,** 1148–1164.

Reasor, P. D., M. D. Eastin, and J. F. Gamache, 2009: Rapidly intensifying Hurricane Guillermo (1997). Part I: Low-wavenumber structure and evolution. *Mon. Wea. Rev.,* **137,** 603–631.

Riehl, H., and J. S. Malkus, 1958: On the heat balance in the equatorial trough zone. *Geophysica,* **6,** 503–538.

——, and ——, 1961: Some aspects of Hurricane Daisy, 1958. *Tellus,* **13,** 181–213.

Rogers, R., 2010: Convective-scale structure and evolution during a high-resolution simulation of tropical cyclone rapid intensification. *J. Atmos. Sci.,* **67,** 44–70.

——, P. Reasor, and S. Lorsolo, 2013: Airborne Doppler observations of the inner-core structural differences between intensifying and steady-state tropical cyclones. *Mon. Wea. Rev.,* **141,** 2970–2991.

Rotunno, R., and J. B. Klemp, 1982: The influence of the shear-induced pressure gradient on thunderstorm motion. *Mon. Wea. Rev.,* **110,** 136–151.

——, and ——, 1985: On the rotation and propagation of simulated supercell thunderstorms. *J. Atmos. Sci.,* **42,** 271–292.

Sampson, C. R., J. Kaplan, J. A. Knaff, M. DeMaria, and C. A. Sisko, 2011: A deterministic rapid intensification aid. *Wea. Forecasting,* **26,** 579–585.

Schubert, W. H., M. T. Montgomery, R. K. Taft, T. A. Guinn, S. R. Fulton, J. P. Kossin, and J. P. Edwards, 1999: Polygonal eyewalls, asymmetric eye contraction, and potential vorticity mixing in hurricanes. *J. Atmos. Sci.,* **56,** 1197–1223.

Shapiro, L. J., and H. E. Willoughby, 1982: The response of balanced hurricanes to local sources of heat and momentum. *J. Atmos. Sci.,* **39,** 378–394.

Sitkowski, M., and G. M. Barnes, 2009: Low-level thermodynamic, kinematic, and reflectivity fields of Hurricane Guillermo (1997) during rapid intensification. *Mon. Wea. Rev.,* **137,** 645–663.

Stern, D. P., and D. S. Nolan, 2011: On the vertical decay rate of the maximum tangential winds in tropical cyclones. *J. Atmos. Sci.,* **68,** 2073–2094.

Stewart, S. R., and S. W. Lyons, 1996: A WSR-88D radar view of Tropical Cyclone Ed. *Wea. Forecasting,* **11,** 115–135.

——, J. Simpson, and D. Wolff, 1997: Convectively-induced mesocyclonic vortices in the eyewall of tropical cyclones as seen by WSR-88D Doppler radars. Preprints, *22nd Conf. on Hurricanes and Tropical Meteorology,* Fort Collins, CO, Amer. Meteor. Soc., 106–108.

van Tassel, E. L., 1955: The North Platte Valley tornado outbreak of June 27, 1955. *Mon. Wea. Rev.,* **83,** 255–264.

Vigh, J. L., and W. H. Schubert, 2009: Rapid development of the tropical cyclone warm core. *J. Atmos. Sci.,* **66,** 3335–3350.

Weisman, M. L., and J. B. Klemp, 1982: The dependence of numerically simulated convective storms on vertical wind shear and buoyancy. *Mon. Wea. Rev.,* **110,** 504–520.

——, and ——, 1986: Characteristics of isolated convective storms. *Mesoscale Meteorology and Forecasting,* P. S. Ray, Ed., Amer. Meteor. Soc., 341–358.

——, and R. Rotunno, 2000: The use of vertical wind shear versus helicity in interpreting supercell dynamics. *J. Atmos. Sci.,* **57,** 1452–1472.

Wilhelmson, R. B., and J. B. Klemp, 1978: A numerical study of storm splitting that leads to long-lived storms. *J. Atmos. Sci.,* **35,** 1974–1986.

Willoughby, H. E., 1990: Temporal changes of the primary circulation in tropical cyclones. *J. Atmos. Sci.,* **47,** 242–264.

——, 1998: Tropical cyclone eye thermodynamics. *Mon. Wea. Rev.,* **126,** 3053–3067.

——, H.-L. Jin, S. J. Lord, and J. M. Piotrowicz, 1984: Hurricane structure and evolution as simulated by an axisymmetric, nonhydrostatic numerical model. *J. Atmos. Sci.,* **41,** 1169–1186.